YU ISSN 0015—3206
FZKAAA 20 (1) 13 (1988)

OXYGEN INTERACTION WITH METAL SURFACES: SURFACE SCIENCE APPROACH

KLAUS WANDELT

Fritz-Haber-Institut der Max-Planck-Gesellschaft, Faradayweg 4—6, D-1000 Berlin 33, F. R. G.

and

PETAR PERVAN and MILORAD MILUN

Institute of Physics of the University, P. O. Box 304, 41001 Zagreb, Yugoslavia

Received 12 December 1987

UDC 538.971

Original scientific paper

A description of the so-called »surface science approach« to systematic studies of oxygen adsorption and surface oxidation is presented by giving a brief review of the use of surface sensitive techniques such as Auger Electron Spectroscopy, Photoelectron Spectroscopy, Low Energy Electron Diffraction and Thermal Desorption Spectrometry in order to study the geometric and electronic structure of chemisorbed oxygen as well as surface oxide layers. Representative results are discussed (in the order of increasing complexity) for single-crystal single-component surfaces, single-crystal binary alloy surfaces, polycristalline single-component surfaces and polycrystalline binary alloy surfaces. New results for the interaction of oxygen with a polycrystalline palladium foil are included in the discussion.

1. Introduction

The interaction of oxygen with metallic surfaces is of fundamental technological and economical importance. Oxygen adsorption constitutes an elementary step in the formation of oxides, in corrosion processes, in catalytic oxidation reactions etc. In the USA an estimated 40% of the annual steel production are only to replace corroded parts. In turn, the controlled formation of thin oxide films plays an im-

portant role for protective passivation and coatings, for insulation in microelectronics and (in future) for thin film superconductors. Ceramics are oxides; and oxidation catalysts are important for pollution control.

In order to understand and control these global processes a detailed insight into the elementary reaction steps on the molecular level is required. This microscopic insight can be obtained by the so-called »surface science approach«: Under ultrahigh vacuum (UHV) conditions ($< 10^{-8}$ Pa) atomically clean metal surfaces are exposed to well defined doses of pure oxygen. The uptake and nature as well as the kinetics and energetics of the metal-oxygen interaction is then studied with highly surface sensitive analytical methods as a function of external parameters such as exposure, pressure and temperature as well as the surface composition and structure. The samples may range from single-component single-crystals to multicomponent polycrystalline surfaces. The surface specific analytical methods generally employed are based on the use of low energy (< 3 keV) electron and ion beams (see Fig. 1), because these particles exhibit only very short ($\sim$1—2 nm)

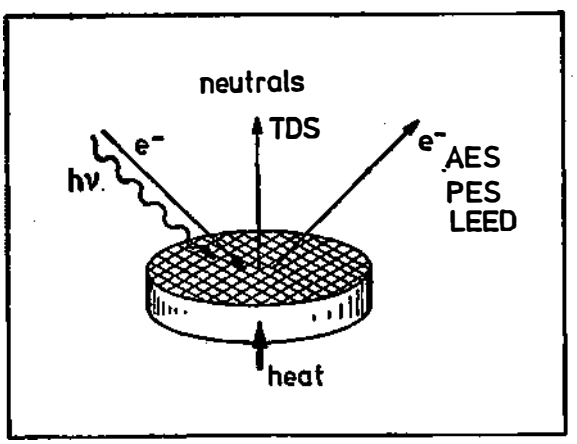

Fig. 1. Illustration of the so-called »surface science approach« for the investigation of the properties of solid surfaces. The surface is exposed, for instance, to beams of primary electrons and photons of different energy. The energetic and spatial distributions of emitted secondary electrons from the surface carry information about the qualitative and quantitative composition of the surface as well as about the crystallographic and electronic structure. Simple heating of the sample may lead to desorption characteristics of adsorbed particles, which are typical for the nature of the adsorption bond.

mean free path lengths in metals. For Auger Electron Spectroscopy (AES) the sample is bombarded with primary electrons of 2—3 keV energy, which causes the emission of secondary electrons from the surface. The spectrum, that is the intensity versus energy curve, of these electrons is detected with an energy dispersive analyzer and contains characteristic signals arising from electronic Auger processes in atoms near the surface. Since such an Auger process involves three intra-atomic electron levels, any Auger signal is denoted by a triplet such as KLL, LMV etc., which means for instance, that an initially created hole state in the K--shell is filled by an electron from the L-shell, and that the energy gain of this transition leads to emission of another L-electron, which is detected. Auger signals

provide qualitative and quantitative information about the chemical nature of the surface (see Figs. 4 and 16). Photoelectron Spectroscopy (PES) to a first approximation is based on a single electron process: The surface is irradiated with soft X-rays (XPS) of e. g. 1253.6 eV (MgKα) or 1486.6 eV (AlKα) energy or with UV-light (UPS) of e. g. 21.22 eV (He I) or $h\nu = 40.81$ eV (He II) energy, which again causes the emission of characteristic electrons. The kinetic energy E_K of these electrons is measured and is given by $E_K = h\nu - \varphi - E_B$. Since the energy of the primary photons $h\nu$ and the work function φ are known, atom-specific electron binding energies E_B can be determined, and the signal intensity is again a quantitative measure of the respective atomic species (see Figs. 3, 5 and 8). Finally, due to the wave nature of electrons, coherent beams of low energy electrons (20—1000 eV) are diffracted by the regular lattice of a single crystal surface. The diffracted beams are made visible by means of a fluorescence screen and form a so-called LEED (low energy electron diffraction) pattern which shows the crystallographic symmetry of the surface (see e. g. Fig. 7). Simple heating of the sample may lead to thermally induced desorption of adsorbed surface species; in Thermal Desorption Spectrometry (TDS) the desorbing species are monitored with a mass-spectrometer and the temperature at which desorption occurs reflects the adsorptive bonding strength. For more detailed information about the methods mentioned the reader is refered to the Refs. 1—3. The intent of the present contribution is to review briefly the use of these surface sensitive techniques in order to investigate some kinetic, energetic, structural and electronic aspects of the oxygen-metal interaction.

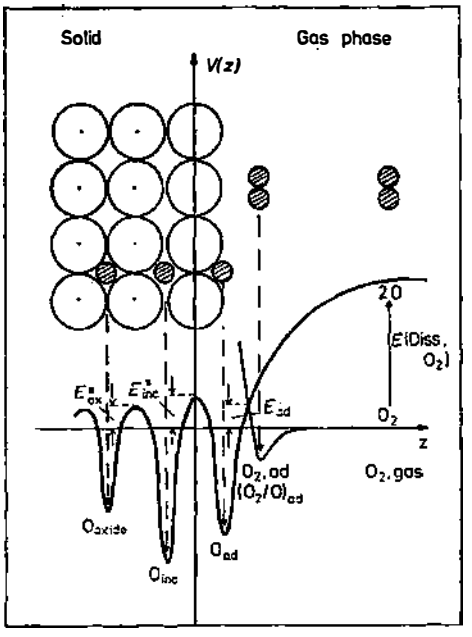

Fig. 2. Schematic representation of the potential energy of an oxygen molecule (or oxygen atom) approaching a surface along the surface normal (z-axis). An oxygen molecule may be trapped in a shallow »physisorption« minimum (O_2, ad) if the activation energy E_{ad}^* for »chemisorption« into the deeper O_{ad}-minimum is positive. Likewise[3], activation barriers E_{inc}^* and E_{ox}^* will control the incorporation of atomic oxygen below the surface or into the final bulk oxide.

Fig. 2 illustrates the various possible interaction channels between oxygen and a metal in the form of a diagram: potential energy V versus (vertical) distance z between a gas-phase oxygen molecule and the metal surface ($z = 0$). At large oxygen-surface separation ($z \to \infty$) the interaction is zero; $V(\infty) = 0$ is taken to be the energy reference. Dissociation of an oxygen molecule in the gas phase »costs« the dissociation energy $E(\text{Diss}, O_2)$. Approach and chemisorptive adsorption of the two obtained oxygen atoms lowers the total energy of the combined system by $E(\text{Diss}, O_2) + 2E(O_{ad})$ (see Fig. 2). The energy gain of $E(O_{ad})$ per atom is the driving force for atomic oxygen adsorption O_{ad} *on* the metal surface. If the oxygen is not predissociated in the gas phase the oxygen molecule O_2 approaches the surface nearly along the z-axis and may be »trapped« in molecular form by a physisorptive energy minimum (O_2, ad) being held by long-range van der Waals forces. Thermal activation of the thus physisorbed O_2 molecule over the »activation barrier« E^*_{ad} may then again lead to dissociative chemisorption into the O_{ad}-minimum at shorter bond distance. In this direct process the activation energy E_{ad} is much smaller than $E(\text{Diss}, O_2)$ in the previous case and $O_{2,ad}$ may be regarded as a »precursor« for chemisorption into the final-state. In fact, E_{ad} may even be negative, so that the intermediate $O_{2,ad}$-state can not be isolated. O_2 physisorption may also occur above surface regions which are already covered by atomic oxygen (see $(O_2/O)_{ad}$ state in Fig. 2). Eventually the metal-oxygen interaction may lead to the formation of thick oxide films and bulk oxides, which means that oxygen atoms are incorporated (O_{inc}) below the surface or bound in deeper layers to form a metal oxide (O_{oxide}). These processes are again controlled by the occurence of corresponding activation barriers, E^*_{inc} and E^*_{ox}, and energy minima of O_{inc} and O_{oxide}. The »surface science approach« allows to investigate the formation and the characteristics of these various stages of oxygen-metal interaction[4].

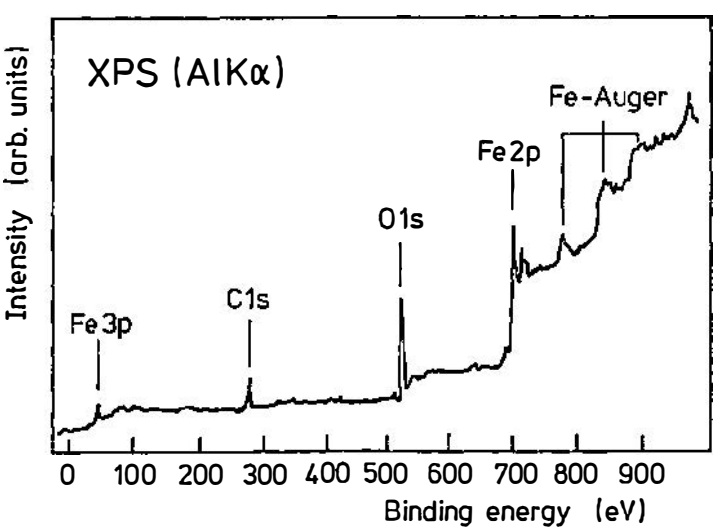

Fig. 3. XPS spectrum (intensity versus energy curve) of an iron surface excited with photons of 1486.6 eV (AlK-radiation). The various peaks correspond to the emission of Fe (3p)-, C (1s)-, O (1s)-, Fe (2p)- and Fe-Auger electrons. The binding energy is refered to the Fermi level of the sample. The presence of the C (1s)- and O (1s)-signal points to surface contamination by carbon and oxygen.

2. *Representative results*

2.1. *Single-component single-crystal surfaces*

Fig. 3 shows the X-ray excited photoelectron (XPS) spectrum (electron intensity versus binding energy) of a carbon (C) and oxygen (O) contaminated iron (Fe) surface. The origin of the energy axis corresponds to the Fermi level E_F of the metal substrate. The peaks correspond to direct Fe (3p)-, C (1s)- and Fe (2p)-core electron or Fe (Auger)-electron emission. The intensity (height) of the C (1s) and O (1s) signal is a quantitative measure of the concentration of these surface contaminants; a few percent of a monolayer can easily be detected. Fig. 4 displays the AES spectrum of a nickel (Ni) surface which is again heavily contaminated with carbon (C) and oxygen (O) (see curve a)). Ion bombardment of this sample under UHV-conditions finally may lead to a nickel surface the AES spectrum of which shows only signals corresponding to pure Ni (curve b)). (The triplets MVV, KLL, LVV, etc. designate Auger electron transitions characteristic of the corresponding chemical species[1-3,5].) The presence of only a few percent of a monolayer of any surface species can again be easily detected by this spectroscopy.

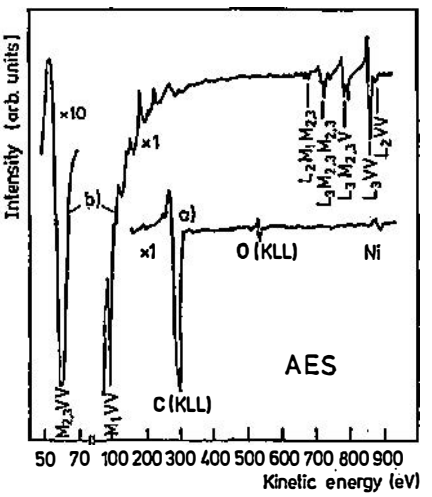

Fig. 4. Auger electron spectrum (AES) of a heavily oxygen (O) and carbon (C) contaminated nickel (Ni) surface (a) and of the same surface after cleaning (b). The triplets KLL, MVV, etc. denote the respective Auger transitions (see text).

The thus prepared atomically clean metal surface can then be exposed to controlled doses of oxygen gas (exposures are measured in units of 1 Langmuir (L) = $= 1\,s \cdot 1.33 \cdot 10^{-4}$ Pa, and the amount of oxygen adsorbed on the surface can be detected, for instance, by the intensity of the O (1s) core electron emission peak. A set of O (1s) signals as measured at 300K sample temperature are shown in Fig. 5. Fig. 6 shows a plot of the O (1s) intensity as a function of oxygen exposure (in Langmuir) to a (100)-oriented single-crystal surface of nickel at 300K. The O (1s) intensity increases rapidly at low exposures (regime), goes through

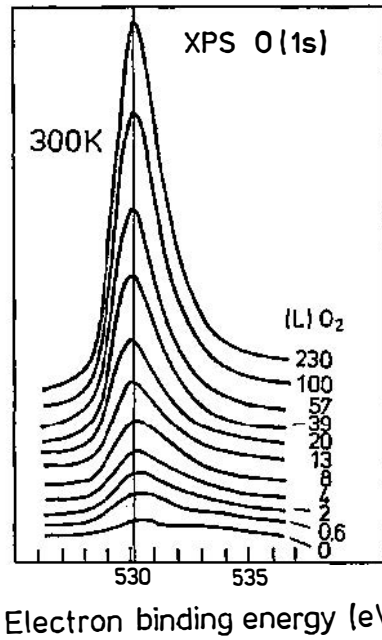

Fig. 5. O (1s) XPS peak of oxygen adsorbed on nickel at room temperature. The intensity of the peak is proportional to the amount of adsorbed oxygen which in turn is a function of the oxygen exposure.

a plateau between ~5L and ~50L (regime II), and then continues to rise less steeply (regime III). The O (1s) intensity is a measure of the number of adsorbed loxygen atoms, while the exposure is proportional to the number of oxygen molecu-$_s$es impinging on the surface, not all of which necessarily stick to the surface. The $_e$ticking coefficient s is thus given by the derivative (slope) of the intensity vs. $_x$posure curve. While the sticking coefficient s_0 (exposure $\rightarrow 0$) is assumed to be ^{u}nity[6] it decreases to $s = 5 \cdot 10^{-3}$ between ~5L and ~50L, and re-increases to $s = 7 \cdot 10^{-2}$ around 100L exposure. A detailed statistical analysis of this variation of s suggests that one impinging O_2 molecule requires a cluster of 8 empty Ni sites on the surface in order to adsorb dissociatively[7].

The three exposure regimes are also characterized by the occurrence of different oxygen-induced extra spots in the corresponding LEED-pattern of the surface. In the first regime (at very low exposures) a so-called p (2 × 2) LEED picture is observed as sketched in Fig. 7, while a c (2 × 2) LEED picture (see Fig. 7) is typical for the regime between ~5L and ~50L (plateau). Beyond 50L any regular diffraction pattern fades away. This latter regime corresponds to the incorporation of oxygen and the formation of bulk nickel oxide (NiO), while the first two exposure regimes correspond to oxygen atoms adsorbed in registry *on* the Ni (100) surface (see Fig. 7). This can be concluded from valence band photoelectron spectra (excited with UV-photons of 21.22 eV; UV-photoelectron spectroscopy (UPS)). An example is shown in Fig. 8[8], where spectrum a) corresponds to the valence electron emission of a clean Ni (1 11) surface. At moderate oxygen exposures (10L)

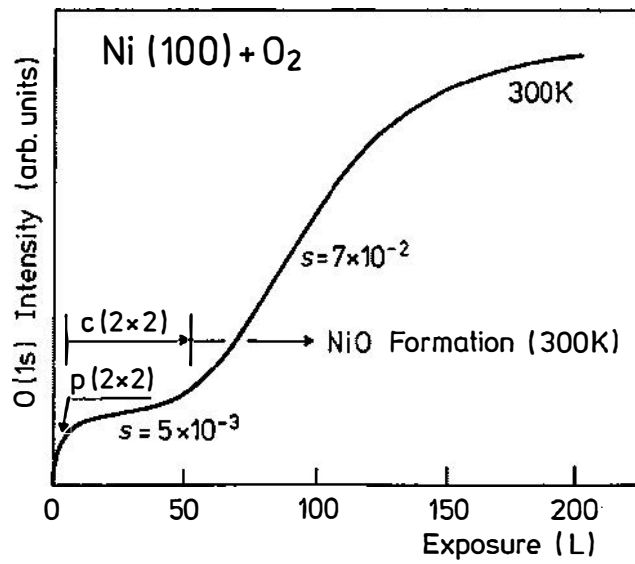

Fig. 6. Plot of the O (1s) intensity as a function of oxygen exposure to a Ni (100) surface at 300K. s denotes the sticking coefficient (see text) and p (2 × 2) and c (2 × 2) refer to the observed LEED pattern (see Fig. 7) in the respective exposure regime.

the leading signal hardly changes, indicating no strong electronic interaction of the oxygen with the Ni (3d) valence electrons. Only the growth of a small peak at 6 eV below E_F due to emission of O (2p) electrons indicates the presence of adsorbed oxygen atoms *on* the surface. After higher exposures (e. g. 100L) the spectrum changes drastically (see curve c), and now corresponds to a superposition of spectra from bulk NiO (see curve d) and from the Ni (111) surface covered with adsorbed oxygen. Very similar data are obtained for the Ni (100) surface.

A combination of such UPS data with the LEED observation from Ni (100) suggests that for the first two exposure regimes oxygen atoms are adsorbed on the Ni (100) surface in p (2 × 2) and c (2 × 2) registry with the substrate surface lattice. This, however still leaves open, the relative lateral orientation between the Ni-surface lattice and the O_{ad}-adsorbate lattice. Three possible models are shown for both the p (2 × 2) and the c (2 × 2) structures in Fig. 7 in which the oxygen atoms are placed, for instance, »ontop« of a nickel atom, in the »hollow-position« between four nickel atoms, or in the »bridge-position« between two Ni-atoms. Additional information is required to pin-down the true location, which can be obtained (besides from LEED-intensity measurements) from angular resolved PES studies. Figs. 9 a) and d), show azimuthal anisotropies of the O (1s) and Cu ($2p_{3/2}$) photoemission intensities as measured from a Cu (100) surface, covered with a c (2 × 2) oxygen overlayer, at a polar emission angle of $\Theta = 13°$ off the surface (see top sketch in Fig. 9) by rotating the crystal by 360° about the surface normal[9]. After subtraction of the respective isotropic background I_{min} the characteristic anisotropies are accentuated in Figs. 9 b) and e). Finally, in order to minimize spurious experimental sources of anisotropy like surface imperfections and heterogeneous fields around the sample, the pattern b) and e) are fourfold averaged

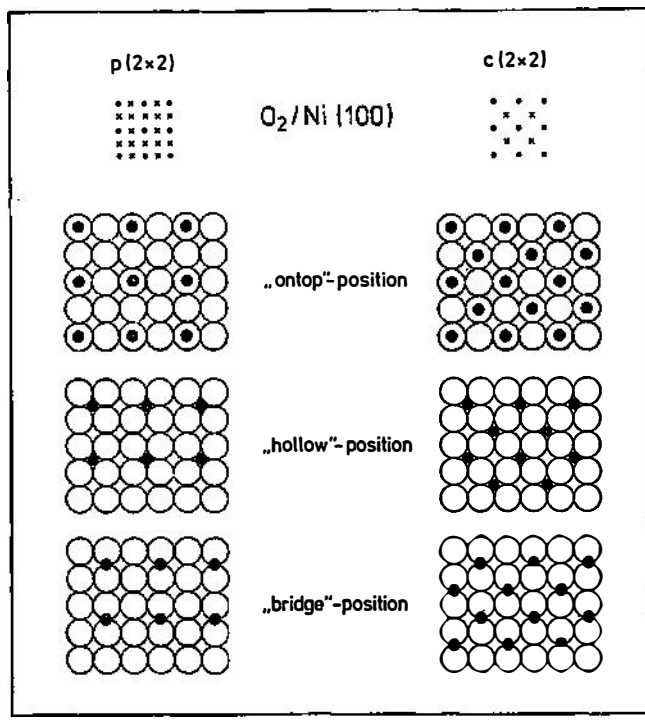

Fig. 7. LEED (Low Energy Electron Diffraction) pattern (reciprocal lattice) and structure models of the p (2 × 2) and c (2 × 2) oxygen adsorption structures on Ni (100). In the LEED pattern (top) the full dots represent the Ni-substrate lattice, the crosses are oxygen induced extra spots. The structure models (below) illustrate possible positions for the oxygen atoms (black), namely ontop of a nickel atom (white), in the hollow between four nickel atoms or in the bridge position between two nickel atoms.

through $\overline{I(\Phi)} = I(\Phi) + I(\Phi + 90°) + I(\Phi + 180°) + I(\Phi + 270°)$ resulting in the appealing »flower patterns« of Fig. 9 c) and f). These latter azimuthal intensity distributions exhibit excellent fourfold symmetry with maxima in the Cu ($2p_{3/2}$) emission coinciding with minima of the O (1s) distribution. The fourfold symmetry appears immediately incompatible with oxygen atoms (being the source of the O (1s) emission) in bridge-positions which exhibit twofold symmetry (see Fig. 7). A detailed analysis, namely of azimuthal anisotropies measured at different polar angles Θ, in fact, suggest that the oxygen atoms occupy fourfold hollow-sites[4]. Fig. 10 illustrates a superposition of the O (1s) pattern from Fig. 9 c) with a atomistic model showing the oxygen atoms in hollow-sites between four Cu-atoms. Intensity maxima are pointing in the direction of »valleys« between adjacent Cu-atoms, which, indeed, may be regarded as the most natural »channels« for electron emission. The same kind of reasoning rules out the »on-top«-position (see Fig. 7).

The reason why the adsorbed oxygen atoms prefer to sit in the hollow-sites is obvious: The fourfold coordination results in the highest chemical bonding strength (four bonds). This argument based on the coordination number is supported by chemisorption theory. Fig. 11 displays the threedimensional plot of a theo-

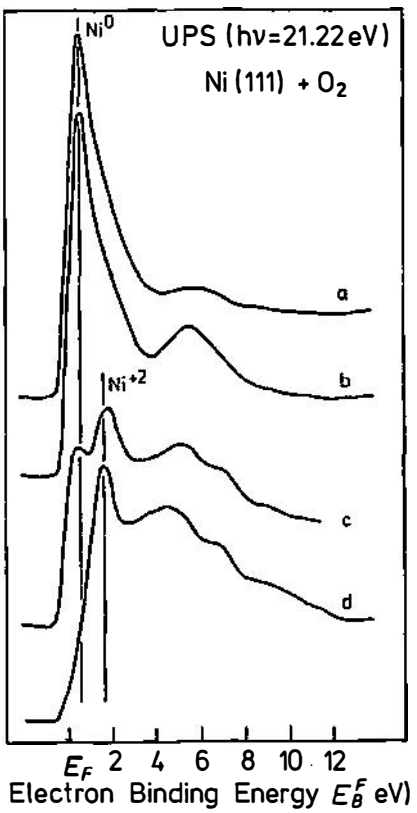

Fig. 8. Representative UPS valence band spectra of a) a clean Ni (111) surface; b) after adsorption of 6L O_2; c) after adsorption of 100L O_2, and d) of bulk NiO.

retically[10] calculated adsorption energy (E_{ad}) hypersurface for various positions of an oxygen atom within as quare unit cell between four Ni surface atoms (see inset). Minima in this hypersurface correspond to sites of highest energy gain and, hence, highest bond strength. Such calculations mainly yield *relative* adsorption energies, and Fig. 11 clearly suggests stronger adsorption between the four Ni-atoms than ontop of a Ni-atom (at each corner). The *absolute* bonding energy of an oxygen atom in the most favourable adsorption site can be determined by means of Thermal Desorption Spectrometry (TDS) as mentioned in the Introduction.

2.2. *Single-component poly-crystalline surfaces*

Of course, differently oriented single-crystal surfaces offer sites of different adsorption symmetry and coordination, and, hence, different relative adsorption energy. In this respect, a single-component, but poly-crystalline surface represents a structurally heterogeneous surface with crystallites of different crystallographic orientation as well as defects in the form of grain boundaries. Adsorbed

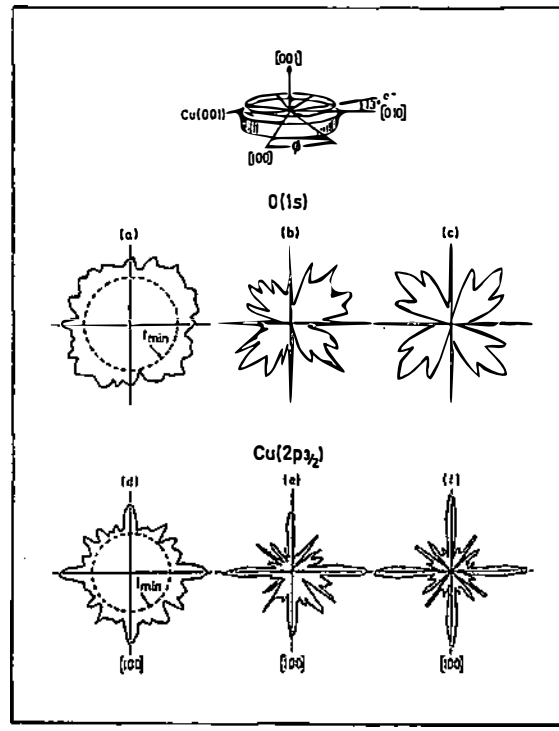

Fig. 9. Azimuthal angular distributions of absolute XPS intensities for the O (1s) (a) and Cu ($2p_{3/2}$) (d) core levels from a Cu (100) surface exposed to 1200L oxygen. A polar emission angle of 13° with respect to the surface was used. The O (1s) data are a sum of three complete scans; Cu ($2p_{3/2}$) is one single scan In (b) and (e), the minimum value I_{min} has been subtracted from the data in order to amplify anisotropies. In (c) and (f) the data have been fourfold averaged (see text) in order to reduce spurious sources of non-fourfold anisotropy (Kono et al.[9]).

oxygen atoms, always seeking for sites of highest adsorption energy, will populate such a polycrystalline surface (as a function of increasing coverage) in the order of decreasing E_{ad}. This appears, indeed, to be reflected in the set of TDS spectra of oxygen from polycrystalline palladium (Pd) shown in Fig. 12a) and b). The polycrystalline Pd foil was first exposed to a given amount of oxygen at 510K[11]. Its temperature was then raised linearly and the partial pressure of desorbing molecular oxygen was monitored as a function of sample temperature. Fig. 12a) shows such desorption curves for initial coverages O_0 as given in the figure. The continuous shift of the curve maximum to lower desorption temperature is compatible with the above notion of the successive population of surface sites in the order of decreasing E_{ad}. Fig. 12b) represents a continuation of Fig. 12a); at these higher coverages Θ_0 with $0.20 < \Theta_0 < 0.5$ of oxygen the desorption traces even begin to show features which are characteristic for oxygen desorption from Pd (110) and Pd (100) single crystal surfaces, suggesting the presence of such patches at the surface of this polycrystalline foil. Analysis of the temperatures corresponding to the peak maxima in Fig. 12a) using established methods[12] yield an initial adsorption energy of $E_{ad} = 230$ kJ/mole at $\Theta_0 < 0.1$. This value is of the same order of magnitude as the one calculated theoretically in Fig. 11.

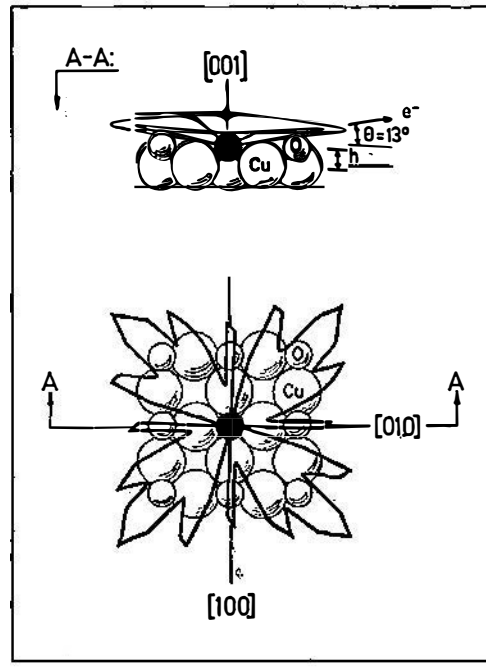

Fig. 10. Side- and top-view of an $O_{ad}c(2 \times 2)$/Cu (100) structure model showing the geometry of detection of the O (1s)- and Cu ($2p_{3/2}$)-azimuthal anisotropies (top) and a superposition of the O (1s)-anisotropy on a fourfold hollow site (bottom).

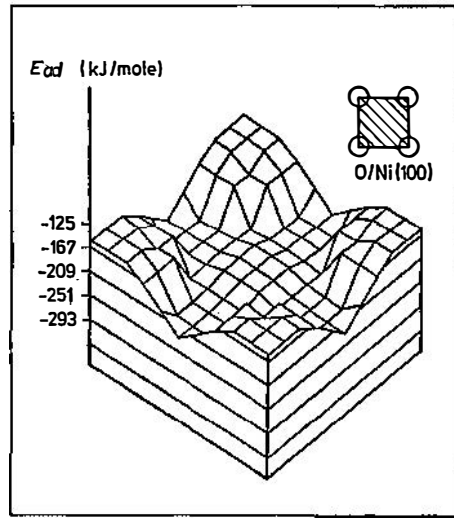

Fig. 11. Theoretically calculated adsorption energy (E_{ad}) hypersurface for different positions o an oxygen atom within a square unit cell between 4 Ni atoms.

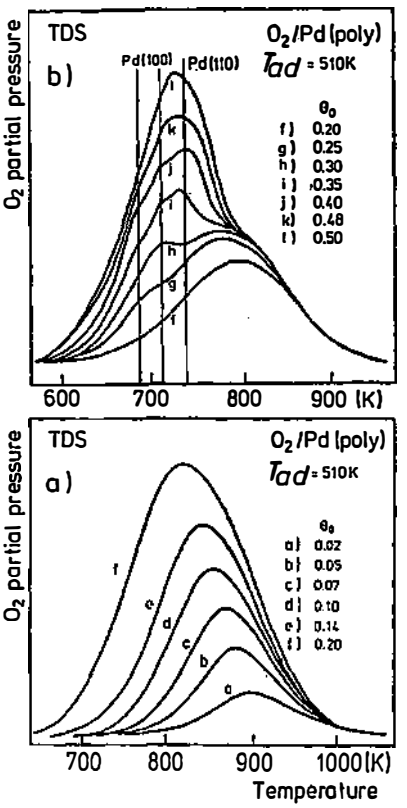

Fig. 12. Thermal desorption spectra of oxygen from a Pd foil after adsorption of different amounts of O_2 at 510K. Θ_0 denotes the initial oxygen coverage. Panel b) is a continuation from panel a).

2.3. *Two-component single-crystal surfaces*

Fig. 13 reproduces[13] $2p_{3/2}$ core level electron spectra of Ni and Fe from a (100) surface of a 76%Ni24%Fe alloy single crystal which was exposed to oxygen at room temperature (curves a)) and then heated to ~600 K without further oxygen supply (curves b)). After *saturating* the surface with oxygen at room temperature the Ni ($2p_{3/2}$) signal shows two peaks which correspond to Ni^{2+}-ions of the NiO overlayer formed and to metallic nickel (Ni^0) underneath. In turn, the Fe ($2p_{3/2}$) signal exhibits only one peak corresponding to Fe^{3+}-ions of the iron oxide. The absence of an Fe^0-signal indicates that the iron component is completely oxidized, in contrast to the nickel near the surface. Heating this surface oxygenated at room temperature to ~600 K leads to significant spectral changes. The nickel oxide is quantitatively reduced to metallic nickel and the oxygen is transfered to iron resulting in more iron oxide formation. Note the loss of the Ni^{2+} signal and the increase of the Fe^{3+} intensity. This transformation is in agreement with the higher heat of formation of (any) iron oxide than that of nickel oxide.

The assignment of the peaks in Fig. 13 to Ni^0, Ni^{2+}, Fe^0, Fe^{3+}, of course, is based on reference measurements with pure nickel and iron as well as with various

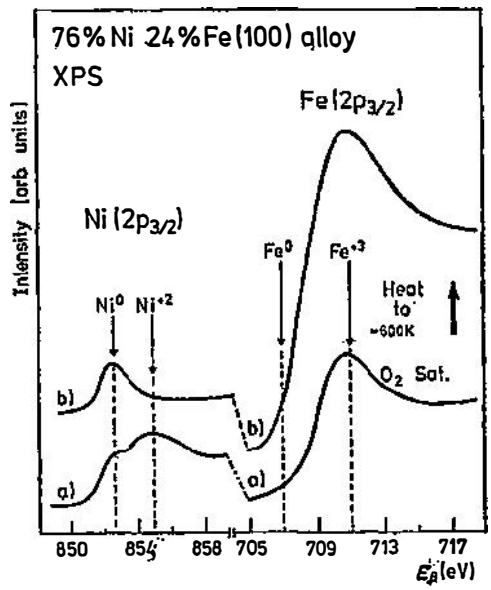

Fig. 13 XPS Ni ($2p_{3/2}$)- and Fe ($2p_{3/2}$)-spectra from the (100) surface of a 76%Fe24%Ni single crystal alloy a) after saturation with oxygen at 300K and b) following heating of this surface to 600K (after Brundle et al.[13]).

possible oxide samples (standards). The detection of such »standard spectra«, however, is much less trivial as it may appear[14]. For instance, iron is known to form three different stable oxides, Fe_xO ($x \approx 0.95$), Fe_3O_4 and Fe_2O_3. Because of their different content of Fe^{2+} and Fe^{3+}-ions one may expect characteristic differences between the Fe ($2p_{3/2}$) photoemission spectra. Fig. 14 shows Fe ($2p_{3/2}$) spectra from various commercial iron oxide samples inserted into the spectrometer as received. The spectra look disappointingly similar; the peak maxima occur at very similar electron binding energies, solely the Fe_xO spectrum shows some deviations in the intensity distribution (see arrows). It has been shown, that the similarity of these spectra arises from the simple fact, that all *air-exposed* oxide surfaces are covered with a layer of the same oxide, namely α-Fe_2O_3, because it is the thermodynamically most stable one. The true reference spectra of the different iron oxides could only be measured if single-crystal samples were crushed or cleaved in situ or under an inert (oxygen-free) argon atmosphere prior to measurement[4]. The thus obtained standard spectra are shown in Fig. 15 (full lines). In these spectra not only the Fe^{2+}-ions of Fe_xO are clearly distinguishable by their $2p_{3/2}$ peak shift, but also the presence of *both* kinds of ions in Fe_3O_4 manifests itself by the occurence of the pronounced Fe^{2+}-shoulder within the low energy edge of the Fe^{3+} peak.

A comparison of these standard spectra (full lines in Fig. 15) with those from Fig. 14 seems to suggest that simple removal of the Fe_2O_3-overlayer from all air-exposed iron oxides should enable the detection of the desired standard spectra. The most frequently employed technique to remove disturbing and contaminating overlayers is ion-bombardment. The surface is exposed to a beam of inert gas ions (e. g. Ar^+) of 1—3 keV energy, and this ion beam »erodes« surface material away.

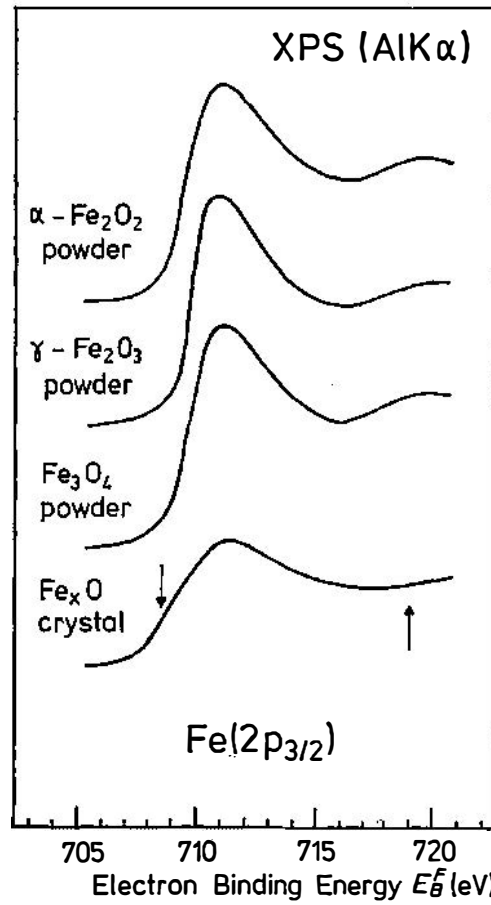

Fig. 14. XPS Fe ($2p_{3/2}$) core level spectra of various iron oxides, taken from the air-exposed samples as received.

This so-called »sputtering« method, however, has the serious disadvantage, that the sputter-coefficient (number of removed surface atoms per incident ion) strongly depends on the atomic mass of the sputtered surface species. For a given ion mass and energy, lighter surface atoms are sputtered more easily than heavier surface atoms. This means in the present case that the lighter oxygen atoms are sputtered more efficiently than the heavier iron atoms. Consequently, the substrate stoichiometry is seriously modified. This becomes most apparent from a comparison between the full and dashed curves in Fig. 15. As mentioned before the full lines are the standard spectra of the single-crystalline and stoichiometric oxides Fe_xO Fe_3O_4 and α-Fe_2O_3, while the dashed spectra were monitored from the same samples after a few minutes of argon ion bombardment. In all cases intensity is shifted to lower electron binding energies corresponding to the emission from lower valent states of iron, namely Fe^{2+} and even metallic Fe^0. These new spectra have no resemblance what so ever with the original (standard) spectra of the stoi-

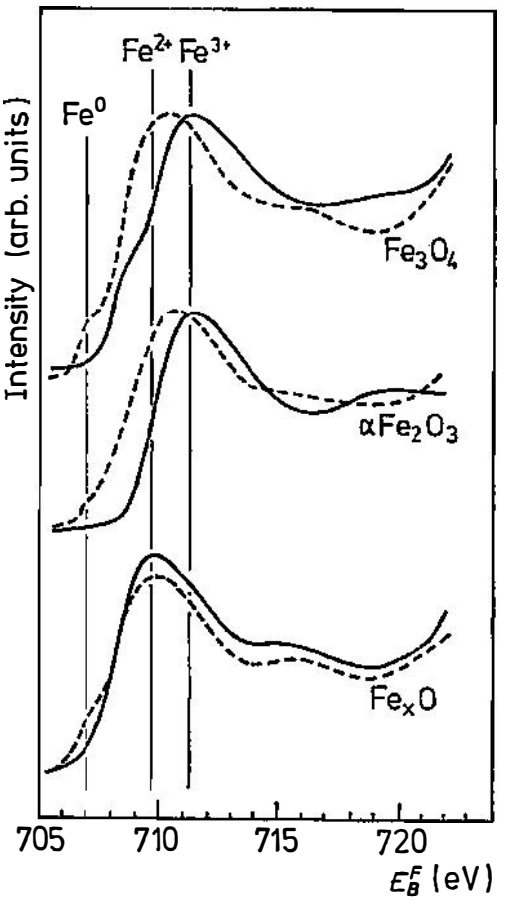

Fig. 15. High resolution Fe ($2p_{3/2}$) XPS spectra showing the effect of Ar^+ bombardment (1keV, 10μA) on iron oxide surfaces The full lines are the standard spectra from the perfect single crystal oxides. The dashed spectra are measured with the bombarded surfaces: Fe_3O_4, Ar^+ for 10 min; Fe_2O_3, Ar^+ for 7 min; Fe_xO, Ar^+ for 3 min).

chiometric starting materials. In view of such dramatic modifications of the surface composition due to selective sputter effects spectra from ion-bombarded multi-component surfaces and, in particular, the interpretation of composition profiles normal to surfaces of multi-component samples must be regarded with extreme caution (if not doubt).

2.4. *Two-component polycrystalline samples*

In this paragraph we carry the discussion one final step further towards an understanding of the interaction of oxygen with more realistic surfaces, namely *poly*crystalline surfaces of *binary* alloys[4,14]. The upper spectrum in Fig. 15 corresponds to the Auger electron spectrum (AES) of a clean polycrystalline 69% Ni 31%Fe alloy surface. This composition is determined from the relative intensity of

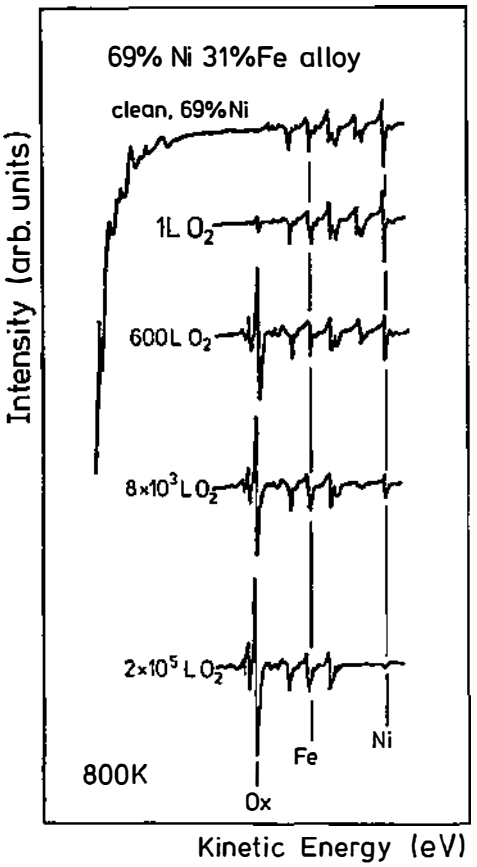

Fig. 16. Auger spectra of a successively oxidized polycrystalline 69%Ni31%Fe sample. The oxidation was performed at 800K and $7.3 \cdot 10^{-3}$ Pa O_2.

the Ni- and Fe-AES signals (see Fig. 16). The surface was then heated to ~800 K and exposed to increasing doses of oxygen gas: the exposures are given in the figure. The spectra exhibit a strong oxygen signal (Ox), but simultaneously the Ni- and Fe-signals show significant changes in relative intensity. The Fe-signal increases slightly while the Ni-signal finally fades away. This observation is in agreement with that from Fig. 13 and suggests segregation of iron oxide to the surface. This iron oxide eventually grows to such a thickness that due to the finite information depth of the emitted Auger electrons the metallic nickel from the alloy underneath is no longer seen. Fig. 17 finally shows a plot of the Fe/Ox- and Ni/Ox--Auger intensity ratios as obtained after heavy oxidation at 800 K of polycrystalline FeNi alloys of different composition. This plot suggests that alloys with an initial nickel concentration of less than 60—70% are finally covered with an overlayer of pure iron oxide, namely Fe_2O_3, while alloy samples containing more than 60——70% nickel are finally covered with an overlayer of Ni-ferrite, which contains both Ni- and Fe-ions. The enhanced enrichment of iron oxide at the surface is

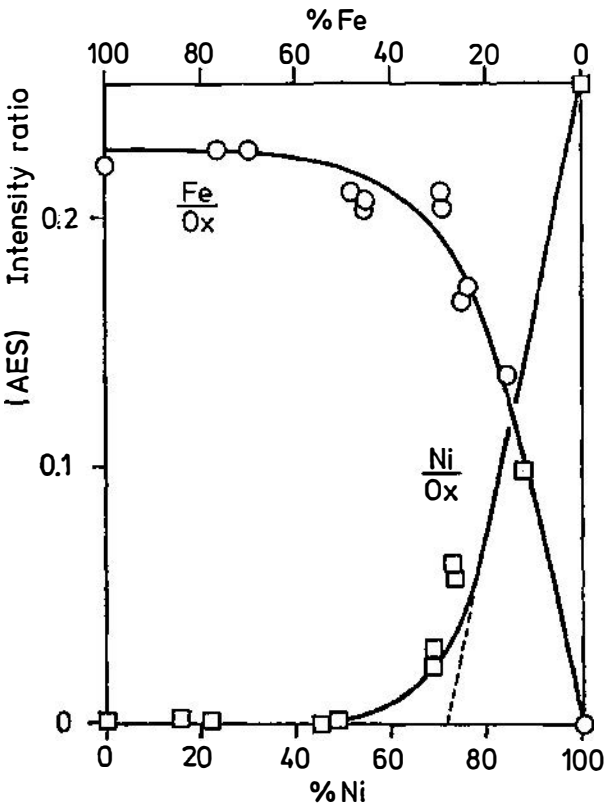

Fig. 17. Ratios of the Auger peak heights Fe (650)/O (515) and Ni (850)/O (515) of completely oxidized NiFe alloys as a function of the initial alloy composition. Oxidation was performed at 800K and $7.3 \cdot 10^{-3}$ Pa O_2.

again expected due to the higher heat of formation of (any) iron oxide than that of nickel oxide. Such stable surface oxides may play an important role as passivation layers which protect the metallic material against further corrosive attack.

3. *Concluding remarks*

In this paper we have presented a brief outline of the so-called »surface science approach« to systematic oxidation studies of metallic surfaces. The examples were chosen in the order of increasing complexity. The simplest and therefore most defined case is the adsorption of oxygen on well defined single-crystal surfaces of pure metals. In this case the structural, electronic and vibrational (not discussed here) properties of adsorbed oxygen atoms can be determined in great detail using various surface sensitive spectroscopies. The results of these well-defined model studies may then serve to understand the oxidation process at more complex sur-

faces. As such we have addressed polycrystalline surfaces of pure metals (here Pd), binary alloy single-crystal surfaces (here FeNi (100)) and polycrystalline FeNi samples of various compositions. This approach of successive generalization appears to be the only way to reach ultimately an understanding of surface oxidation in particular, and corrosion in general.

Acknowledgements

This work was in part supported by both the BMFT through the Internationales Büro of the KFA — Jülich, and the SIZ za znanstveni rad SRH, through the ZAMTES office Zagreb, under the auspices of the bilateral Yugoslav—German research project *Surface Physics*, No. 32.2.A.F., as well as by the Deutsche Forschungsgemeinschaft through Sonderforschungsbereich 128 (München) and 6 (Berlin) and the SIZ za znanstveni rad SRH (Project 24.8). The International Atomic Energy Agency, Vienna, supported part of this work through the research contracts No. 3227 and 4527. The authors are also indebted to G. Ertl, C. R. Brundle, G. Doyen and C. S. Fadley for the permission to use their figures.

References

1) *Practical Surface Analysis*, Eds. D. Briggs and M. P. Seah (John Wiley and Sons, New York, 1983);
2) D. P. Woodruff and T. A. Delchar, *Modern Techniques of Surface Science* (Cambridge University Press, 1986);
3) G. Ertl and J. Küppers, *Low Energy Electrons and Surface Chemistry* (Verlag Chemie, Weinheim, 1985);
4) K. Wandelt, *Photoemission Studies of Adsorbed Oxygen and Oxide Layers*, Surface Sci. Rep. **2** (1982) 1, and references therein;
5) R. Weissmann and K. Müller, *Auger Electron Spectroscopy — A Local Probe for Solid Surfaces*, Surface Sci. Rep. **1** (1981) 251;
6) C. R. Brundle and H. Hopster, J. Vac. Sci. Technol. **18** (1981) 63;
7) C. R. Brundle, R. J. Behm and J. A. Barker, J. Vac. Sci. Technol. **A2** (1984) 1038;
8) H. Conrad, G. Ertl, J. Küppers and E. E. Latta, Solid State Commun. **17** (1975) 497;
9) S. Kono, C. S. Fadley, N. F. T. Hall and Z. Hussain, Phys. Rev. Lett. **41** (1978) 117;
10) G. Doyen, Ph. D. — Thesis, München, 1975;
11) M. Milun, P. Pervan and K. Wandelt, Surface Sci. **189/190** (1987) 466;
12) The relevant methods have been refered to and discussed in:
a) P. Pervan and M. Milun, Fizika **18** (1986) 47;
b) P. Pervan, M. Milun and K. Wandelt, Appl. Surface Sci. **29** (1987) 271;
13) C. R. Brundle, E. Silverman and R. J. Madix, J. Vac. Sci. Technol. **16** (1979) 474;
14) K. Wandelt and G. Ertl, Surface Sci. **55** (1976) 403.

INTERAKCIJA KISIKA S METALNIM POVRŠINAMA

KLAUS WANDELT*, PETAR PERVAN** i MILORAD MILUN**

* *Fritz-Haber-Institut der Max-Planck-Gesellschaft, Faradayweg 4—6, D-1000 Berlin 33, F. R. G.*

** *Institut za fiziku sveučilišta, p. p. 304, 41001 Zagreb, Jugoslavija*

UDK 538.971

Originalni znanstveni rad

U radu je opisan sistematski pristup istraživanju adsorpcije kisika i oksidacije površina metodama znanosti o površinama. Ukratko je oslikana upotreba površinski osjetljivih eksperimentalnih tehnika kao što su Augerova elektronska spektroskopija, fotoelektronske spektroskopije, difrakcija nisko-energetskih elektrona i termalna desorpcijska spektroskopija u istraživanjima elektronskih i strukturnih karakteristika kemisorbiranog kisika i oksidnih slojeva. Diskutirani su reprezentativni slučajevi za (prema rastućoj složenosti) mono-kristalne jednokomponentne površine, mono-kristalne binarne površine, polikristaliničnе jednokomponentne i dvokomponentne (binarne slitine) površine. Također su u diskusiju uključeni i novi rezultati istraživanja interakcije kisika s polikristaliničnom folijom paladija.